PDT-S-T: A New Polymer with Optimized Molecular Conformation for Controlled Aggregation and π–π Stacking and Its Application in Efficient Photovoltaic Devices

Yue Wu, Zhaojun Li, Wei Ma,* Ye Huang, Lijun Huo,* Xia Guo, Maojie Zhang, Harald Ade, and Jianhui Hou*

In recent years, polymer solar cells (PSCs) have attracted much attention due to their advantages of fabricating low-cost and light-weight solar panels through roll-to-roll printing techniques.[1,2] Until now, significant improvements in power conversion efficiencies (PCEs) have been achieved and PCEs of 8–9% have been realized with conventional, single layer bulk heterojunction (BHJ) solar cells.[3–11] Among various photovoltaic materials for the applications in BHJ PSCs, conjugated polymers based on fused aromatic units are particularly interesting due to their well delocalized π-conjugation along the backbones. In the past a few years, more and more fused aromatic units, like benzodithiophene (BDT),[4,12,13] thieno[3,4-*b*]thiophene (TT),[8] benzodifuran,[14,15] indacenodithiophene (IDT),[16] indacenodithienothiophene (IDTT),[17] dithienosilole (DTS),[18] dithienogermole(DTG),[19] dithienobenzodithiophene (DTBDT),[20] and so on, have been introduced into photovoltaic polymers and contributed a lot to the development of PSCs.[21–25] Besides the design of conjugated polymers with different backbone structures, the modulation of the polymers' molecular energy levels by changing the electron pushing or withdrawing effects of their side groups has also attracted much attention as molecular design motif for photovoltaic polymers. Many excellent examples have been reporting this strategy.[4,5,26]

Molecular configuration and conformation are two important but seldomly investigated structural motifs for molecular design of photovoltaic polymers. The study of regio-regular poly(3-hexylthiophene) (P3HT) provides the first and also the most important example of optimizing molecular configuration to improve photovoltaic properties of conjugated polymer.[27] For example, highly crystalline structure can be formed in the regio-regular P3HT, while the blend of regio-random P3HT is amorphous.[28,29] The crystallization forces favorable morphologies that yield PCE of the PSC based on regio-regular P3HT and PCBM of over 4%,[30,31] which is 2–6 times higher than that of the PSC based on regio-random P3HT and PCBM.[32] In addition to configuration, the morphology of photovoltaic devices might also be affected by the polymer's molecular conformation. For instance, polymers with straight linear backbone structure should be more likely to realize highly crystalline morphology than polymers with branched or zigzagged liner backbones. However, in the molecular design of photovoltaic polymers, the correlation among molecular conformation, the crystallinity of the morphology, propensity for π–π stacking, J- versus H-aggregation, and photovoltaic performance has been seldomly studied possibly due to the lack of model polymer systems.

The low band gap polymer system based on BDT and TT, known as PBDTTTs, exhibited efficient photovoltaic properties.[4,26] Recently, several interesting results related to the molecular design and the application of PBDTTTs in highly efficient PSCs have been reported.[3,33–35] Interestingly, according to the reported results, most of the PBDTTT polymers are amorphous.[34,36] Therefore, figuring out why PBDTTTs are amorphous and then to find a method to improve their crystallinity or π–π stacking through molecular structure design will be helpful to achieve in-depth understanding of photovoltaic polymers. In this work, we tried to use molecular conformation as the root cause to interpret why PBDTTT-S-T (see **Scheme 1**) is amorphous. A new polymer, PDT-S-T as shown in Scheme 1, which has similar molecular structure as PBDTTT-S-T but different backbone conformation, was designed to realize more ordered morphology in thin films. The morphological and photovoltaic results indicate that PDT-S-T exhibits more ordered structure and better photovoltaic properties than PBDTTT-S-T, that is, PCEs of the PSCs based on PBDTTT-S-T and PDT-S-T are 5.93% and 7.79%, respectively. Besides of reporting a new photovoltaic polymer with enhanced photovoltaic performance, we correlate structural characteristics as revealed by X-ray diffraction, tapping mode atomic force microscopy (AFM) and transmission electron microscope (TEM), and photovoltaic performance with the polymers' molecular conformations, and argue that molecular conformation should be considered in photovoltaic polymer design.

As demonstrated in Scheme 1. PBDTTT-S-T has zigzagged linear backbones due to the conformational nature of BDT and

Y. Wu, Z. Li, Y. Huang, Prof. L. Huo, X. Guo,
M. Zhang, Prof. J. Hou
State Key Laboratory of Polymer Physics
and Chemistry
Beijing National Laboratory for Molecular Sciences
Institute of Chemistry
Chinese Academy of Sciences
Beijing 100190, China
E-mail: huolijun@iccas.ac.cn; hjhzlz@iccas.ac.cn
W. Ma, Prof. H. Ade
Department of Physics
North Carolina State University Raleigh
NC 27695, USA
E-mail: wma5@ncsu.edu
Y. Wu, X. Guo
Graduate University of Chinese Academy of Sciences
Beijing 100049, China
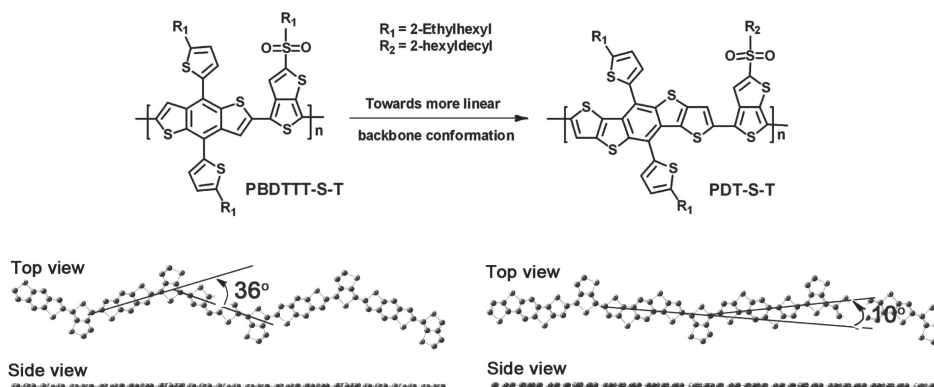
Scheme 1. Molecular structures and backbone conformations of PBDTTT-S-T and PDT-S-T. The molecular conformations of these two backbones are obtained through the density functional theory (DFT) at the B3LYP/6-31G(d,p) level.

TT building blocks and the zigzagged backbone of PBDTTT-S-T shows an angle of 36°, which may have negative influence on realizing crystalline morphology in solid film. On the other hand, the bond angel of C–S–C in the sulfonyl group is 108°, which causes strong steric hindrance to the adjacent side groups, so that the alkyl in the sulfonyl cannot lie in the same plane with the backbone.[34] Therefore, it should be hard to obtain ordered packing in the solid film of PBDTTT-S-T. As demonstrated in Scheme 1, from PBDTTT-S-T to PDT-S-T, the replacement of BDT with DTBDT gives three potential advantages: first, the backbone of PDT-S-T can be arranged with more linear conformation; second, the distance between the adjacent side groups is big enough to allow the alkyls on the sulfonyl groups to keep in the same plane with the backbone; third, the intermolecular π–π stacking of the polymer will be enhanced. Hence, based on the DFT calculations, it can be predicted that both inter-chain packing and inter-planar π–π stacking should be more ordered and intermolecular π–π stacking should be more compact for the solid film of PDT-S-T than for films of PBDTTT-S-T.

The synthesis approaches for these two polymers are shown in **Scheme 2**. The alkoxy-substituted DTBDT(1) was prepared by the method reported in our previous work.[20] Ammonium ceric nitrate (CAN) was used to oxidize the alkoxy-substituted DTBDT(1) in acetonitrile and the corresponding quinone compound (2) can be obtained easily with a yield in 75%. Then, the thienyl-substituted DTBDT monomer (DTBDT-T) can be prepared in high yields by the similar method as used in the synthesis of thienyl-substituted BDT derivatives.[3] The bis(trimethyltin)-BDT monomer (BDT-T) is commercial available. The two dibromo monomers (TT-S1 and TT-S2) were synthesized by the same procedure.[37] The copolymers of PBDTTT-S-T and PDT-S-T were prepared through the Stille coupling reaction between the bis(trimethyltin) monomers (BDT-T and DTBDT-T, respectively) and the dibromo monomers (TT-S1 and TT-S2, respectively) as shown in Scheme 2. These two polymers exhibit good solubility in commonly used organic solvents such as chloroform, toluene, xylenes, and o-dichlorobenzene (o-DCB), as well as good thermal stability below 350 °C under inert atmosphere (see Figure S1, Supporting Information). Through
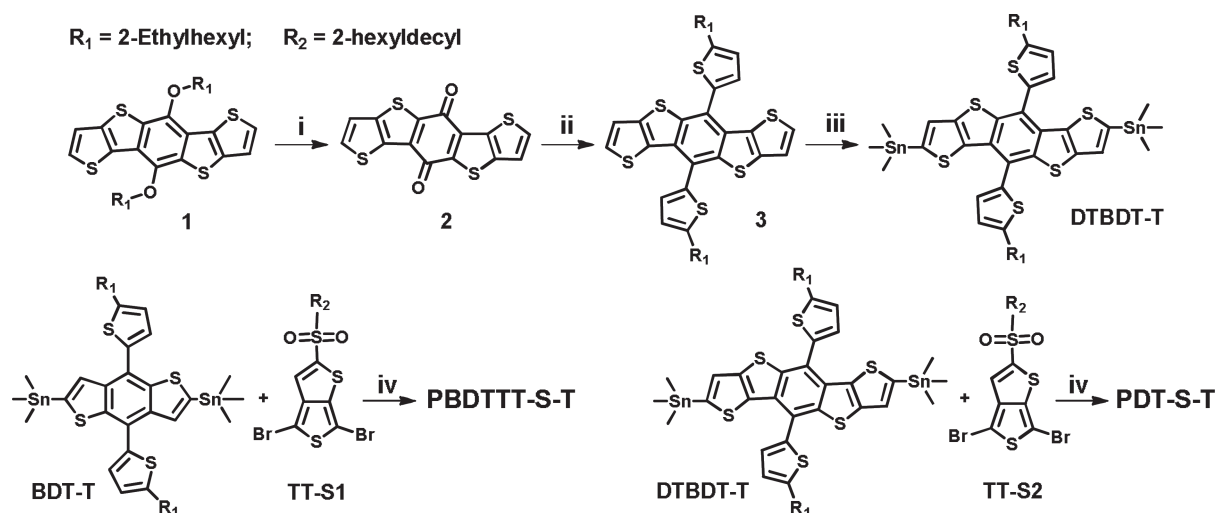
Scheme 2. Synthesis procedures of PBDTTT-S-T and PDT-S-T. i) CAN, acetonitrile, ambient temperature, 1 h; ii) 2-(2-ethylhexyl)-thiophene, butyl-lithium, THF, inert atmosphere, 50 °C, 1 h; then SnCl$_2$, HCl/H$_2$O, inert atmosphere, 50 °C, 1.5 h; iii) LDA, THF, inert atmosphere, −78 °C, 1 h, then trimethyltin chloride, inert atmosphere, ambient temperature, 1 h; iv) Pd(PPh$_3$)$_4$, Toluene/DMF (10:1, v/v), inert atmosphere, reflux, 8 h.
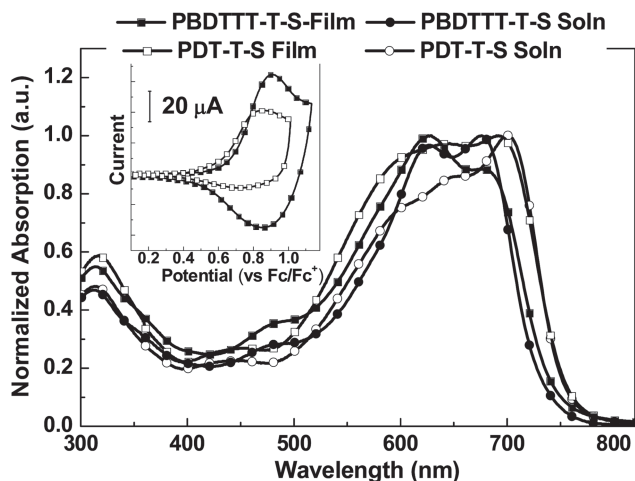
Figure 1. UV-Vis absorption spectra of the solutions in chloroform and the solid films of PBDTTT-S-T and PDT-S-T; Insert: Cyclic voltammogram plots of PBDTTT-S-T and PDT-S-T films on glassy carbon working electrode in 0.1 M Bu_4NPF_6 in CH_3CN at a scan rate of 20 mV s^{-1}.

differential scanning calorimetry (DSC) measurements, we found that no endo- or exothermal signals can be observed in the range of 0–280 °C from the second heating and cooling runs (10 °C min^{-1}).

The ultraviolet-visible (UV–vis) absorption spectra of PBDTTT-S-T and PDT-S-T in diluted solutions and as solid thin films are shown in **Figure 1** and the detailed parameters are colleted in **Table 1**. The solutions and the solid films of these two polymers show almost identical absorption onset at ≈780 nm, corresponding to an optical band gap (E_g^{opt}) of 1.59 eV. The molar extinction coefficients of PBDTTT-S-T and PDT-S-T are 4.57×10^4 M^{-1} cm^{-1}and 4.40×10^4 M^{-1} cm^{-1} respectively, which are among the highest values in organic semiconductors. However, the main absorption peak of PDT-S-T is located at 702 nm, which is red-shifted be ≈30 nm compared to that of PBDTTT-S-T. Interestingly, the absorption in short wavelength direction of PDT-S-T is also extended slightly compared to that of PBDTTT-S-T. Overall, the broader absorption band of PDT-S-T will be beneficial to utilizing more sunlight in PSCs, thus leading to enhanced short circuit current density (J_{sc}) in device. We also note that PDT-S-T is an exceptionally strong J-aggregate in solution (on account of its strong low energy absorption peak), which is slightly reduced on the solid film. This indicates

that molecular design indeed leads to strong coupling along the polymer backbone, requiring the functional groups to stay in a well defined plan without twisting. The reduction on J-aggregate character in the thin film would indicate either twisting due to disorder or increased chain-to-chain coupling, that is, H-aggregation via π–π coupling.

The insert in Figure 1 shows the electrochemical cyclic voltammetry (CV) plots of these two polymers. The onset p-doping potentials (E_{ox}) of PBDTTT-S-T and PDT-S-T are 0.59 V and 0.51 V, corresponding to the highest occupied molecular orbital (HOMO) levels of −5.29 eV and −5.21 eV, respectively.[38] Clearly, the HOMO level of PDT-S-T is slightly higher than that of PBDTTT-S-T, implying that the DTBDT unit may have stronger electron donating effect than the BDT unit. Considering that open circuit voltage (V_{oc}) of PSCs is closely related to the offset between the HOMO level of the electron donor material and the lowest unoccupied molecular orbital (LUMO) level of the electron acceptor material,[12,39] the replacement of BDT with DTBDT should have some negative influence on V_{oc} in PSCs, that is, the PSC based on PDT-S-T might exhibit lower V_{oc} than the PSC based on PBDTTT-S-T.

Grazing incidence X-ray diffraction (GIXD) has been widely used to characterize the formation of ordered structures within the thin films of these two polymers. The two-dimensional GIXD profiles of these two pure polymers are shown in **Figure 2**a and the out-of-plane and the in-plane GIXD profiles extracted from the 2D profiles are provided in Figure 2b. Since the diffraction signal near 1.6–1.9 Å^{-1} is due to the (010) π–π

Table 1. Optical absorption properties and molecular energy level data of the polymers.

Polymer	Solution[a]	Film	E_g^{opt} [eV]	HOMO [eV]	LUMO [eV]
	λ_{max} [nm]/ ε [M^{-1} cm^{-1}]	λ_{onset} [nm]			
PBDTTT-S-T	676/4.57 $\times 10^4$	768	1.61	−5.29	−1.00
PDT-S-T	700/4.40 $\times 10^4$	778	1.59	−5.21	−1.08

[a]in diluted chloroform.
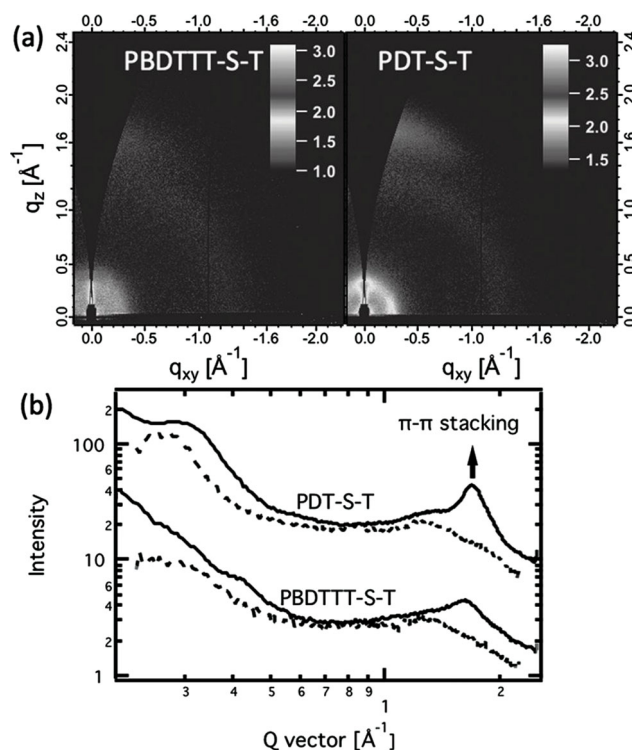
Figure 2. a) GIXD 2D scattering of thin films of PBDTT-S-T and PDT-S-T. b) Out-of plane (solid lines) and in-plane (dashed lines) sector average profiles extracted from (a); GIXD profiles between polymers have been shifted vertically for ease of comparation.

COMMUNICATION

stacking, and both pure films show clear diffraction signal in out-of-plane direction but very weak signal in the in-plane direction, it can be concluded that the molecules in both two pure films are dominantly arranged with face-on structure. In the PBDTTT-S-T, the weak (010) π–π stacking peak is at 1.62 Å^{-1}, corresponding to a d-spacing of 3.88 Å. For the PDT-S-T film, a strong (010) π–π stacking peak at 1.71 Å^{-1} can be observed, corresponding to a d-spacing of 3.67 Å, one of the smallest π–π stacking distances for conjugated polymers observed to date. In the low q range, a (100) peak was observed only for PDT-S-T, which is weak and broad and centered at q $\approx$ 0.32 Å^{-1}, corresponding to a lamellar d-spacing of 19.6 Å. The observation in GIXD measurements clearly indicates that the polymer's molecules can be arranged more ordered by the replacement of BDT with DTBDT, which is consistent with the material design protocol as demonstrated above, that is, the straight linear conformation of the backbone is more favorable to form ordered interchain packing than the zigzagged conformation. Additionally, the reduced steric hindrance between the adjacent alkyl side groups is helpful to get more ordered and also more compact π–π stacking.

The results of the GIXD and the UV-vis measurements shown above can be interpreted as following. As demonstrated in **Scheme 3**, since PBDTTT-S-T has zigzagged linear backbone conformation, ordered inter-chain packing can be formed only under the favorable mode and thus the polymer aggregation will contribute to the (100) peak in GIXD profile. Under the unfavorable mode, the inter-chain distance between the adjacent main chains are varied along the backbones, so that the inter-chain packing will be non-ordered. However, the d-spacing between the adjacent backbones of PDT-S-T is almost constant under the general packing mode, because this polymer has more linear backbone conformation than PBDTTT-S-T, and therefore, the film of PDT-S-T shows a clear (100) peak in the out-of-plane profile of the GIXD analysis. On the other hand, since it is harder to form ordered structure for inter-chain packing in PBDTTT-S-T than PDT-S-T, the ordered inter-chain face-to-face π–π stacking will be definitely weakened in PBDTTT-S-T. Therefore, the PBDTTT-S-T film shows a much weaker (010) scattering peak than the PDT-S-T film in GIXD profile. Although the packing modes shown in Scheme 3 are extreme examples presumed according to the optimized backbone structures, it provides a reasonable interpretation for the different behaviors of these two polymers in GIXD analysis. Overall, the concept that the linearity and the planarity of backbone conformation play important roles in

the formation of ordered morphology for conjugated polymers provides helpful guidance for molecular design of photovoltaic polymers.

Photovoltaic properties of these two polymers were investigated by fabricating PSC devices with a structure of ITO/PEDOT:PSS/Polymer:PC$_{71}$BM/Ca/Al. o-DCB was used to prepare the solutions for spin-coating of active layers and a concentrations of 10 mg mL^{-1} (calculated for polymer) was used in this work. Initially, different donor/acceptor (D/A) ratios (polymer/PC$_{71}$BM, wt/wt), 1:1, 1:1.5 and 1:2, were scanned to find the best weight ratio of device fabrication and the thickness of the active layers used in this work is $\approx$110 nm $\pm$ 5 nm. The current density–voltage (J–V) curves of the PSC devices under the illumination of AM 1.5 G, 100 mW cm^{-2} are shown in **Figure 3**a and the photovoltaic parameters are collected in **Table 2**. When varying the mixture ratio of polymer/PC$_{71}$BM, the values of V_{oc} seems to be depending on the ratio. For PBDTTT-S-T, the V_{oc} varying from 0.83 to 0.81 V and for PDT-S-T, the V_{oc} varying from 0.76 to 0.72 V. The phenomenon is quite similar to the reported works on PIDTDTQx/PCBM and MEH-PPV/PCBM photovoltaic systems. According to the literature reports, this may be caused by the formation of PCBM cluster or increased permittivity.[40,41] From Table 2 it can be seen that the optimum D/A ratio of both copolymers were 1:1.5. Under the optimal donor/acceptor weight ratio, the PSC based on PBDTTT-S-T shows a PCE of 5.0% with J_{sc} = 11.79 mA cm^{-2}, V_{oc} = 0.81 V and FF = 0.52; the PSC based on PDT-S-T exhibited a PCE of 7.79% with J_{sc} = 16.63 mA cm^{-2}, V_{oc} = 0.73 V and FF = 0.64.

Solvent additives, like 1,8-diiodooctane (DIO) and octane-1,8-dithiol (DT), play an important role in optimizing photovoltaic performance of PSCs, and according to the reported works, when PBDTTTs were used as electron donor materials in PSCs, the addition of DIO was always helpful to improve photovoltaic performance of the devices.[4,8,42] Therefore, we used DIO to attempt further improvements in device performance of these two polymers, and different volume ratios of DIO (v/v, DIO/o-DCB), 0.5%, 1%, 2% and 3%, were employed to find the optimal composition of the processing solvent. The J–V curves of the PSC devices prepared by the corresponding solvent mixtures are shown in Figure 3b and the photovoltaic parameters are collected in **Table 3**. Similar to other PBDTTT derivatives, photovoltaic performance of the PBDTTT-S-T devices can also be improved after adding DIO, that is, after adding DIO, both J_{sc} and FF improved but V_{oc} dropped slightly. The champion device (PCE = 5.93%) was obtained when 2% DIO was added. Very interestingly, the blend of PDT-S-T and PC$_{71}$BM show much different behaviors upon the treatment of DIO. As shown in Figure 3b and also listed in Table 3, when the content of the DIO in the solvent was stepwise increased from 0.5% to 3%, FF of the PDT-S-T based device dropped gradually from 0.641 to 0.508 while V_{oc} and J_{sc} of the devices changed a little, and therefore, the overall efficiency dropped to 5.81%. To the best our knowledge, PDT-S-T is the first photovoltaic polymer that exhibits efficient photovoltaic performance above 7% PCE without any further treatment such as use of additives or annealing in device fabrication.
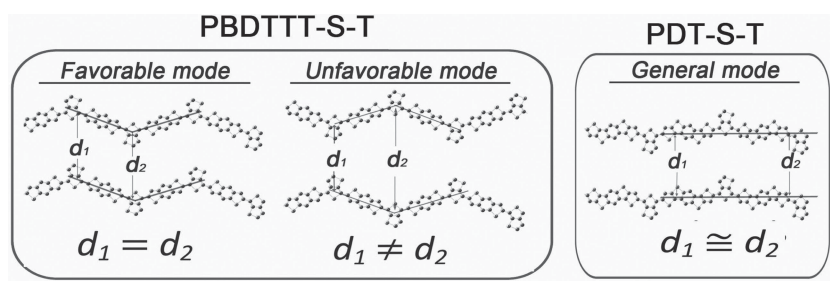
Scheme 3. The demonstration of the top views of the packing modes in PBDTTT-S-T and PDT-S-T.
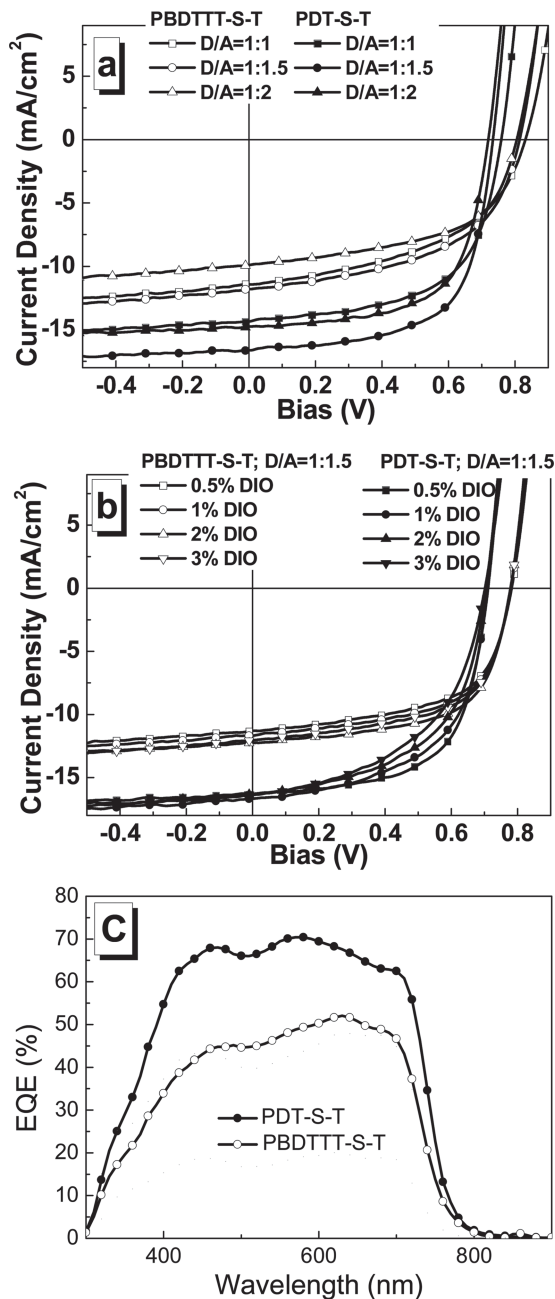
Figure 3. *J*-*V* curves of the PSC devices based on PBDTTT-S-T:PC$_{71}$BM and PDT-S-T:PC$_{71}$BM under the illumination of AM 1.5G 100 mW cm^{-2}; a) the PSC devices processed with different D/A ratios; b) the PSC devices with D/A = 1:1.5 processed by adding different amounts of DIO additive; c) *EQE* curves of the photovoltaic cells of both polymers under prepared by the optimal conditions.

The external quantum efficiency (*EQE*) curves of the two kinds of devices prepared by the optimal conditions are plotted in Figure 3c. It is quite clear that EQE of the PDT-S-T based device is higher in the whole range than that of PBDTTT-S-T based device. According to the EQE curves, the integral current density values of the devices based on PBDTTT-S-T and PDT-S-T are 11.84 mA cm^{-2} and 15.78 mA cm^{-2}, respectively. The mismatch between the integral values and the *J*$_{sc}$ values obtained

Table 2. Photovoltaic results of the PSC devices based on PBDTTT-S-T:PC$_{71}$BM and PDT-S-T:PC$_{71}$BM with different D/A ratios under the illumination of AM 1.5G 100 mW cm^{-2}.

Polymer	D:A	V_{oc} [V]	J_{sc} [mA cm^{-2}]	FF [%]	PCE [%]
PBDTTT-S-T	1:1	0.83	11.41	48.57	4.60
	1:1.5	0.81	11.79	52.12	5.00
	1:2	0.81	9.91	54.92	4.41
PDT-S-T	1:1	0.76	14.36	59.65	6.51
	1:1.5	0.73	16.63	64.13	7.79
	1:2	0.72	14.75	63.48	6.74

from *J*-*V* measurements is within 5%, indicating that the *J*-*V* measurements in this work are reliable.

AFM and TEM were used to investigate the influence of the addition of DIO on the morphology of the blend films. **Figure 4** shows the TEM images of the thin films of PBDTTT-S-T:PC$_{71}$BM and PDT-S-T:PC$_{71}$BM blends. For the PDT-S-T:PC$_{71}$BM blend, when the film was prepared by *o*-DCB only, moderate phase separated morphology are formed (see Figure 4a,b) and the RMS roughness of the film is 0.95 nm; after increasing the volume ratios of DIO in the processing solvent, the blend films show stronger phase separation and greater surface roughness (see Figure 4d,e; Figure S2, Supporting Information). For example, the RMS roughness of the film processed by adding 2% volume ratios of DIO as solvent additive increased to 1.93 nm. According to the TEM images (see Figure 4c,f), when DIO was used as additive, the phase separation in the PDT-S-T/PC$_{71}$BM blend increased slightly. For the PBDTTT-S-T:PC$_{71}$BM blend, when the film was prepared by using only, phase separation in the blend is quite severe so that big size aggregations are formed in the Figure 4i, that is >100 nm dark domains can be observed; when 2% DIO was used as additive to process the blend, the film gives a homogeneous morphology in Figure 4l. The results from AFM and TEM measurements indicate that optimal phase separation can be formed in the PDT-S-T/PC$_{71}$BM blend by using pure as processing solvent, and the use of DIO will induce stronger phase separation as well as rougher surface of the film, resulting in lower photovoltaic performance; however, the morphology of

Table 3. Photovoltaic results of the PSC devices based on PBDTTT-S-T:PC$_{71}$BM (1:1.5) and PDT-S-T:PC$_{71}$BM (1:1.5) processed by adding different amount of DIO under the illumination of AM 1.5G 100 mW cm^{-2}.

Polymer	DIO/*o*-DCB [v/v,%]	V_{oc} [V]	J_{sc} [mA cm^{-2}]	FF [%]	PCE [%]
PBDTTT-S-T	0.5	0.78	11.28	59.30	5.22
	1	0.78	11.33	61.40	5.43
	2	0.78	12.27	61.98	5.93
	3	0.78	12.06	59.97	5.64
PDT-S-T	0.5	0.71	16.38	62.39	7.26
	1	0.71	16.68	56.90	6.74
	2	0.71	16.30	54.88	6.35
	3	0.70	16.32	50.87	5.81
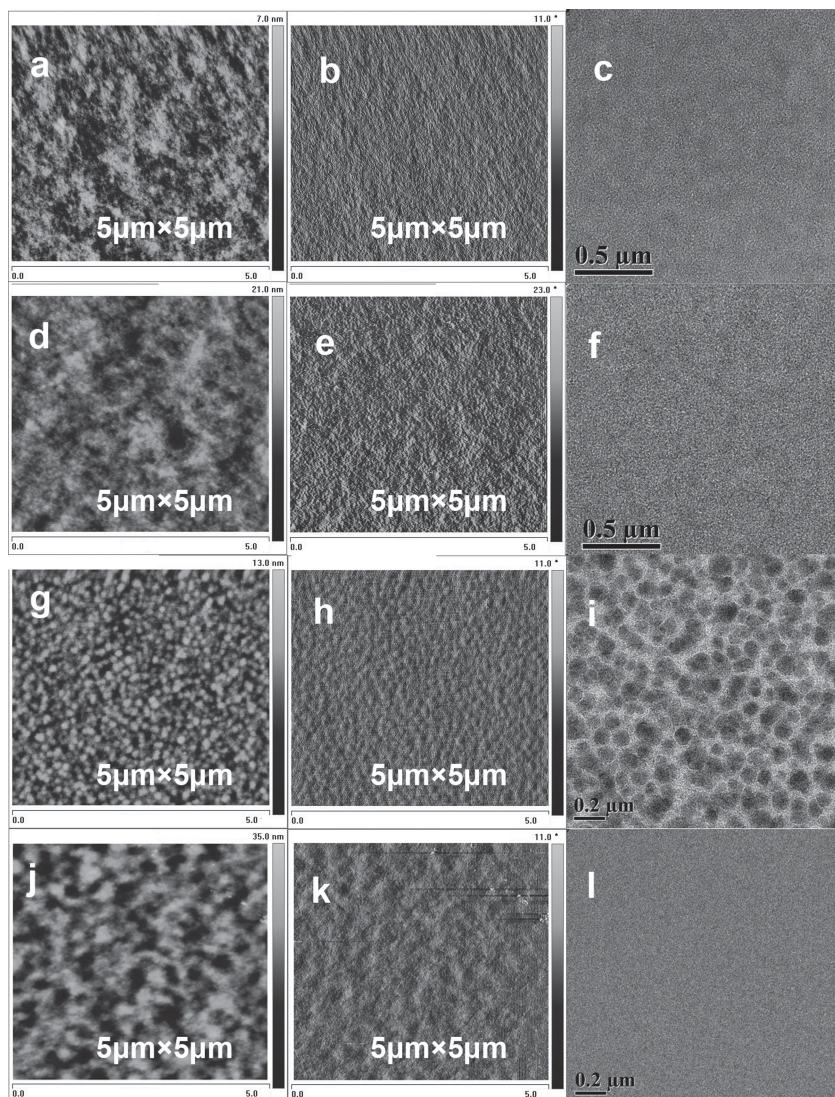
Figure 4. Tapping mode AFM topography, phase and TEM images of a–c) PDT-S-T:PC$_{71}$BM (1:1.5 processed by *o*-DCB), d–f) PDT-S-T:PC$_{71}$BM (1:1.5 processed by *o*-DCB with 2% DIO additive), g–i) PBDTTT-S-T:PC$_{71}$BM (1:1.5 processed by *o*-DCB) and j–l) PBDTTT-S-T:PC$_{71}$BM (1:1.5 processed by *o*-DCB with 2% DIO additive). The size of the AFM images is 5 μm × 5 μm.

shows a higher PCE of 7.79% without using any special treatment, suggesting that more linear backbone would be helpful to improve photovoltaic properties of the photovoltaic polymer. More importantly, since the results clearly shows that morphology and, thus, photovoltaic properties of the conjugated polymers correlate with their molecular conformation closely, the control of molecular conformation would be as a useful tool to modulate photovoltaic properties of conjugated polymers.

Supporting Information

Detailed information for material, instruments, synthesis procedures of the polymers, and device fabrication processes are listed in the Supporting Information, available from the Wiley Online Library or from the author.

Acknowledgements

the blend of PBDTTT-S-T:PC$_{71}$BM can be optimized by adding DIO.

In conclusion, in order to investigate the correlation among polymers' molecular conformation, morphology, and photovoltaic properties, two new modeling polymers, named as PBDTTT-S-T and PDT-S-T, were designed, synthesized, and applied in PSCs. Since the backbone of PDT-S-T has a more linear conformation compared to that of PBDTTT-S-T, more ordered inter-chain packing can be formed in the film of PDT-S-T. On the other hand, from PBDTTT-S-T to PDT-S-T, the distance between the adjacent alkyl side groups is enlarged and, hence, the steric hindrance can be reduced, so that the film of PDT-S-T shows stronger and more compact inter-molecular π–π stacking than that of PBDTTT-S-T. The PSC based on PBDTTT-S-T/PC$_{71}$BM shows a PCE of 5.93% with the use of the additive DIO, while the PSC based on PDT-S-T:PC$_{71}$BM

[1] G. Yu, J. Gao, J. C. Hummelen, F. Wudl, A. J. Heeger, *Science* **1995**, *270*, 1789–1791.

[2] G. Dennler, M. C. Scharber, C. J. Brabec, *Adv. Mater.* **2009**, *21*, 1323–1338.

[3] L. J. Huo, S. Q. Zhang, X. Guo, F. Xu, Y. F. Li, J. H. Hou, *Angew. Chem. Int. Ed.* **2011**, *50*, 9697–9702.

[4] H. Y. Chen, J. H. Hou, S. Q. Zhang, Y. Y. Liang, G. W. Yang, Y. Yang, L. P. Yu, Y. Wu, G. Li, *Nat. Photonics* **2009**, *3*, 649–653.

[5] H. X. Zhou, L. Q. Yang, A. C. Stuart, S. C. Price, S. B. Liu, W. You, *Angew. Chem. Int. Ed.* **2011**, *50*, 2995–2998.

[6] S. C. Price, A. C. Stuart, L. Q. Yang, H. X. Zhou, W. You, *J. Am. Chem. Soc.* **2011**, *133*, 4625–4631.

[7] Z. C. He, C. M. Zhong, X. Huang, W.-Y. Wong, H. B. Wu, L. W. Chen, S. J. Su, Y. Cao, *Adv. Mater.* **2011**, *23*, 4636–4643.

[8] Y. Y. Liang, Z. Xu, J. B. Xia, S.-T. Tsai, Y. Wu, G. Li, C. Ray, L. P. Yu, *Adv. Mater.* **2010**, *22*, E135–E138.

[9] L. T. Dou, J. B. You, J. Yang, C.-C. Chen, Y. J. He, S. Murase, T. Moriarty, K. Emery, G. Li, Y. Yang, *Nat. Photonics* **2012**, *6*, 180–185.

[10] X. Guo, M.J. Zhang, J. H. Tan, S. Q. Zhang, L. J. Huo, W. P. Hu, Y. F. Li, J. J. Hou, *Adv. Mater*, **2012**, *24*, 6536–6541.

[11] T.-Y. Chu, J. P. Lu, S. Beaupre, Y. G. Zhang, J.-R. Pouliot, S. Wakim, J. Y. Zhou, M. Leclerc, Z. Li, J. F. Ding, Y. Tao, *J. Am. Chem. Soc.* **2011**, *133*, 4250–4253.

[12] J. H. Hou, M.-H. Park, S. Q. Zhang, Y. Yao, L.-M. Chen, J.-H. Li, Y. Yang, *Macromolecules* **2008**, *41*, 6012–6018.

[13] L. J. Huo, J. H. Hou, S. Q. Zhang, H.-Y. Chen, Y. Yang, *Angew. Chem. Int. Ed.* **2010**, *49*, 1500–1503.

[14] L. J. Huo, Y. Huang, B. H. Fan, X. Guo, Y. Jing, M. J. Zhang, Y. F. Li, J. H. Hou, *Chem. Commun.* **2012**, *48*, 3318–3320.

[15] L. J. Huo, L. Ye, Y. Wu, Z. J. Li, X. Guo, M. J. Zhang, S. Q. Zhang, J. H. Hou, *Macromolecules* **2012**, *45*, 6923–6929.

[16] I. McCulloch, R. S. Ashraf, L. Biniek, H. Bronstein, C. Combe, J. E. Donaghey, D. I. James, C. B. Nielsen, B. C. Schroeder, W. M. Zhang, *Acc. Chem. Res.* **2012**, *45*, 714–722.

[17] Y.-X. Xu, C.-C. Chueh, H.-L. Yip, F.-Z. Ding, Y.-X. Li, C-Z Li, X. S. Li, W.-C. Chen, A. K.-Y. Jen, *Adv. Mater.* **2012**, *24*, 6356–6361.

[18] J. H. Hou, H. Y. Chen, S. Q. Zhang, G. Li, Y. Yang, *J. Am. Chem. Soc.* **2008**, *130*, 16144–16145.

[19] C. M. Amb, S. Chen, K. R. Graham, J. Subbiah, C. E. Small, F. So, J. R. Reynolds, *J. Am. Chem. Soc.* **2011**, *133*, 10062–10065.

[20] Y. Wu, Z. J. Li, X. Guo, H. L. Fan, L. J. Huo, J. H. Hou, *J. Mater. Chem.* **2012**, *22*, 21362–21365.

[21] C. Chochos, S. Choulis, *Prog. Polym. Sci.* **2011**, *36*, 1362.

[22] Y.-J. Cheng, S.-H. Yang, C.-S. Hsu, *Chem. Rev.* **2009**, *109*, 5868–5923.

[23] B. C. Thompson, J. M. J. Frechet, *Angew. Chem. Int. Ed.* **2008**. *47*, 58–77.

[24] J. W. Chen, Y. Cao, *Acc. Chem. Res.* **2009**, *42*, 1709–1718.

[25] L. J. Huo, J. H. Hou, *Polym. Chem.* **2011**, *2*, 2453.

[26] Y. Y. Liang, D. Q. Feng, Y. Wu, S.-T. Tsai, G. Li, C. Ray, L. P. Yu, *J. Am. Chem. Soc.* **2009**, *131*, 7792–7799.

[27] H. Y. Mao, B. Xu, S. Holdcroft, *Macromolecules* **1993**, *26*, 1163–1169.

[28] G. Barbarella, A. Bonghi, M. Zambianchit, *Macromolecules* **1994**, *27*, 3039–3045.

[29] T.-A. Chen, X. M. Wu, R. D. Rieke *J. Am. Chem. Soc.* **1995**, *117*, 233–244.

[30] G. Li, V. Shrotriya, J. S. Huang, Y. Yao, T. Moriarty, K. Emery, Y. Yang, *Nat. Mater.* **2005**, *4*, 864.

[31] W. L. Ma, C. Y. Yang, X. Gong, K. H. Lee, A. J. Heeger, *Adv. Funct. Mater.* **2005**, *15*, 1617.

[32] Y. Kim S. Cook, S. M. Tuladhar, S. A. Choulis, J. Nelson, J. R. Durrant, D. D. C. Bradley, M. Giles, I. Mcculloch, C.-S. Ha, M. Ree, *Nat. Mater.* **2006**, *5*, 197–203.

[33] Z. C. He, C. M. Zhong, S. J. Su, M. Xu, H. B. Wu, Y. Cao, *Nat. Photonics* **2012**, *6*, 591–595.

[34] Y. Huang, X. Guo, F. Liu, L. J. Huo, Y. N. Chen, T. P. Russell, C. C. Han, Y. F. Li, J. H. Hou, *Adv. Mater.* **2012**, *24*, 3383–3389.

[35] X. H. Li, W. C. H. Choy, L. J. Huo, F. X. Xie, W. E. I. Sha, B. F. Ding, X. Guo, Y. F. Li, J. H. Hou, J. B. You, Y. Yang, *Adv. Mater.* **2012**, *24*, 3046–3052.

[36] M. R. Hammond, R. J. Kline, A. A. Herzing, L. J. Richter, D. S. Germack, H.-W. Ro, C. L. Soles, D. A. Fischer, T. Xu, L. Yu, M. F. Toney, D. M. DeLongchamp, *ACS Nano* **2011**, *5*, 8248–8257.

[37] Y. Huang, L. J. Huo, S. Q. Zhang, X. Guo, C. C. Han, Y. F. Li, J. H. Hou, *Chem. Commun.* **2011**, *47*, 8904–8906.

[38] J. H. Hou, Z. A. Tan, Y. Yan, Y. J. He, C. H. Yang, Y. F. Li, *J. Am. Chem. Soc.* **2006**, *128*, 4911–4916.

[39] M. C. Scharber, D. Mhlbacher, M. Koppe, P. Denk, C. Waldauf, A. J. Heeger, C. J. Brabec, *Adv. Mater.* **2006**, *18*, 789.

[40] K. Vandewal, A. Gadisa, W. D. Oosterbaan, S. Bertho, F. Banishoeib, I. V. Severen, L. Lutsen, T. J. Cleij, D. Vanderzande, J. V. Manca, *Adv. Funct. Mater.* **2008**, *18*, 2064–2070.

[41] D. Veldman, Ö. İpek, S. C. J. Meskers, J. Sweelssen, M. M. Koetse, S. C. Veenstra, J. M. Kroon, S. S. van Bavel, Joachim Loos, R. A. J. Janssen, *J. Am. Chem. Soc.* **2008**, *130*, 7721–7735.

[42] J. Peet, J. Y. Kim, N. E. Coates, W. L. Ma, D. Moses, A. J. Heeger, G. C. Bazan, *Nat. Mater.* **2007**, *6*, 497–500.